Alkali-feldspar separation

The standard alkali-feldspar separation procedure includes two steps of heavy liquid separation at 2.62 and 2.58 gr cm^{-3} (Aitken et al., 1998) and is time consuming. In order to make the separation procedure more efficient, other separation methods were explored. Two samples from the Kerem Shalom (KR) section (KR-7, KR-9) were separated by three different methods: a standard two-step separation with heavy liquids (procedure A); magnetic separation through a LB-1 Frantz magnetic separator, using a current of 1.4 A on the magnet, followed by a one-step heavy liquid separation of the nonmagnetic fraction at 2.58 gr cm^{-3} (procedure B); or the magnetic fraction at the same density (procedure C). All the density-separated fractions lighter than 2.58 gr cm^{-3} were etched for 10 min with 10% HF solution (Porat et al., 2015) and measured with the pIR-IR_{290} protocol (Table 2 in the main text; average of 6 aliquots) and were analyzed with the Scanning electron microscope (SEM).

For both samples, the *De* values obtained from measuring aliquots separated with procedures B and C are, within errors, similar (Table S1). SEM mapping showed that all the separated fractions are mostly composed of quartz, K-feldspar and Na-feldspar minerals with variable proportions (Fig. S1). Element mapping showed that for procedure B, the grains were mostly K-feldspar minerals (Fig. S1), almost identical to the grains separated with procedure A. On the other hand, there were significantly less K-feldspar mineral grains separated with procedure C. Therefore, procedure B, with one-step density separation at 2.58 gr cm^{-3} following magnetic separation, was selected for K-feldspar grains extraction. The heavy fraction of this separation was farther used for quartz extraction.

Table S1: PIR-IR_{290} *De* values measured for samples KR-7 and KR-9 separated by the different procedures. N=6.

Sample	**Separation procedure**	***OD* (%)**	***De* (Gy)**
KR-7	A	17	168±29
	B	6	161±12
	C	1	196±7
KR-9	A	5	194±12
	B	10	224±27
	C	10	226±28

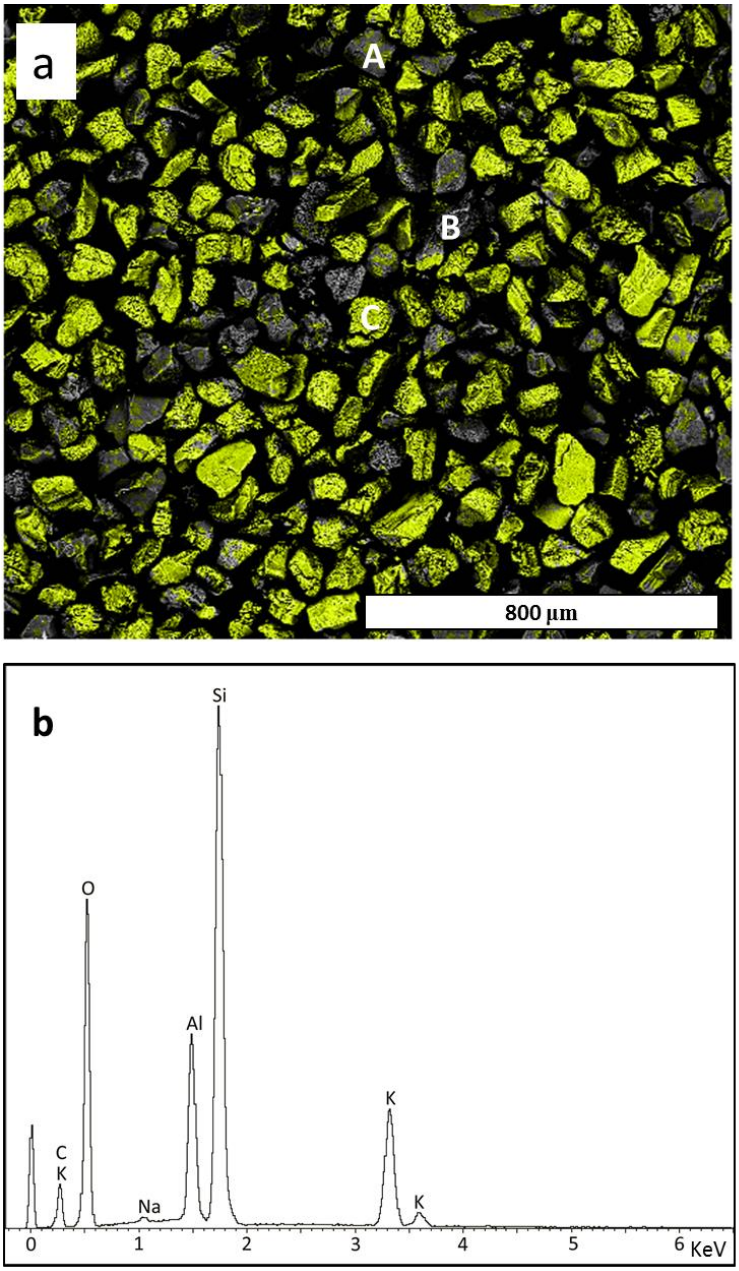

Figure S1: SEM results of sample KR-7 separated using procedure B. a) SEM image of the sample. Grains rich with potassium are colored in yellow. The sample contains Na-feldspar (A) quartz (B) K- feldspar (C – the majority of grains). B) SEM EDS composition spectra of mineral grain C indicating K-feldspar composition.

Table S2: Details of additional samples used in the study for various experiments. All samples are of aeolian sediments originated from the Nile.

Sample	**site**	**Mineral**	**Grain size (μm)**	**Source**	**Remarks**
DF-13	Negev Dune field	quartz	150-177	Roskin et al., 2011	OSL age 40±10 a
ML-D-13	Shefayim	feldspar	150-177	Geological Survey of Israel (GSI) luminescence laboratory unpublished data	Modern beach sample
RUH-40	Ruhama	quartz	90-125	GSI luminescence laboratory unpublished data	TT-OSL *De* 42±2 Gy
RUH-90	Ruhama	quartz	90-125	GSI luminescence laboratory unpublished data	TT-OSL *De* 53±3 Gy
RUH-180	Ruhama	quartz	90-125	GSI luminescence laboratory unpublished data	TT-OSL *De* 163±15 Gy
RUH-300	Ruhama	quartz	90-125	GSI luminescence laboratory unpublished data	TT-OSL *De* 264±11 Gy

Table S3: VSL MAAD ages. The *Ln/Tn* values of the KR samples were projected onto the MAAD DRC constructed for the modern quartz sample DF-13 fitted with one exponential plus linear and two exponentials functions.

				1exp+linear function		**2exp function**	
sample	**depth (m)**	**Dose rate (μGy a^{-1})**	***Ln/Tn***	***De* (Gy)**	**Age (ka)**	***De* (Gy)**	**Age (ka)**
KR-1	15.3	680±45	0.70±0.05	815±260	1200±382	773^{+5256}_{-498}	1137^{+7730}_{-732}
KR-2	12.5	680±44	0.63±0.13	458±511	674±751	429^{+6208}_{-155}	631^{+9130}_{-229}
KR-3	10.7	1052±62	0.51±0.09	149±133	141±126	170^{+362}_{-87}	162^{+344}_{-82}
KR-4	6.3	1560±80	0.49±0.07	130±57	83±37	144^{+243}_{-90}	92^{+156}_{-58}
KR-5	4.1	1319±73	0.46±0.05	108±29	82±22	113^{+161}_{-82}	85^{+122}_{-62}
KR-6	1.5	1218±65	0.22±0.09	29±18	24±14	24^{+43}_{-10}	20^{+35}_{-8}
KR-7	2.3	1598±77	0.29±0.05	45±12	28±8	40^{+53}_{-29}	25^{+33}_{-18}
KR-8	3	1556±75	0.42±0.02	87±8	56±5	85^{+96}_{-76}	55^{+62}_{-49}
KR-9	4.1	1232±66	0.48±0.07	121±51	98±42	131^{+221}_{-83}	106^{+179}_{-67}
KR-10	5.2	1363±74	0.57±0.07	227±175	166±128	265^{+449}_{-155}	194^{+329}_{-114}
KR-11	5.8	1538±79	0.69±0.10	785±514	510±334	726^{+6215}_{-320}	472^{+4041}_{-208}
KR-12	7.2	1698±88	0.61±0.08	352±296	208±174	361^{+693}_{-196}	213^{+408}_{-115}
KR-13	8.2	1014±48	0.64±0.05	508±240	501±237	462^{+705}_{-317}	456^{+696}_{-313}
KR-14	9.5	1273±78	0.72±0.07	954±370	749±291	1094^{+6064}_{-518}	860^{+4763}_{-407}
KR-15	11.7	730±44	0.70±0.10	826±526	1131±720	788^{+6256}_{-337}	1080^{+8570}_{-462}
KR-16	1.5	1200±62	0.15±0.02	17±3	14±3	13^{+17}_{-10}	11^{+14}_{-9}
DF-13			0.02±0.01				

References:

Aitken, M.J., 1998. An Introduction to Optical Dating: the Dating of Quaternary Sediments by the Use of Photon-stimulated Luminescence. Oxford University Press.

Porat, N., Faershtein, G., Medialdea, A., Murray, A.S., 2015. Re-examination of common extraction and purification methods of quartz and feldspar for luminescence dating. Ancient TL 33, 22-30.

Roskin, J., Porat, N., Tsoar, H., Blumberg, D.G., Zander, A.M., 2011. Age, origin and climatic controls on vegetated linear dunes in the northwestern Negev Desert (Israel). Quaternary Science Reviews 30, 1649-1674.